This is a non-peer reviewed preprint submitted to EarthArXiv.

Assessing vertical accuracy and spatial coverage of ICESat-2 and GEDI spaceborne lidar for creating global terrain models

Maarten Pronk[a,b,*], Hugo Ledoux[b], Marieke Eleveld[a,b]

[a] *Deltares; P.O. Box 177, 2600 MH Delft, The Netherlands*
[b] *TU Delft; P.O. Box 5, 2600 AA Delft, The Netherlands*

Abstract

Digital elevation models (DEMs) are a necessity for modelling many large-scale environmental processes. In this study, we investigate the potential of data from two spaceborne lidar altimetry missions, ICESat-2 and GEDI—with respect to their vertical accuracies and planimetric data collection patterns—as sources for rasterisation towards global DEMs. We validate the terrain measurements of both missions against airborne lidar datasets over three areas in the Netherlands, Switzerland, and New Zealand, and differentiate them using landcover classes. For our experiments, we use three and a half years of ICESat-2 ATL03 data and three years of GEDI L2A data, totalling 252 million measurements. The datasets are filtered using parameter flags provided by the higher-level products, respectively ICESat-2 ATL08 and GEDI L3A. For all areas and land cover classes combined, ICESat-2 achieves a bias of −0.11 m, a MAE of 0.43 m, and a RMSE of 0.93 m. From our experiments, we find that GEDI is less accurate with a bias of 0.09 m, a MAE of 0.98 m and a RMSE of 2.96 m. Measurements in open land cover classes, such as "Cropland" and "Grassland", result in the best precision for both missions. We also find that the slope of the terrain is a major influence on vertical accuracy, and more so for GEDI than ICESat-2, because of its larger horizontal geolocation error. Contrastingly, we find little effect of either beam power or background solar radiation, nor do we find noticeable seasonal effects on accuracy. Furthermore, we investigate the spatial coverage of ICESat-2 and GEDI by deriving a DEM at different horizontal resolutions and latitudes. GEDI has higher spatial coverage than ICESat-2 at lower latitudes due to its beam pattern and lower inclination angle, and a derived DEM can achieve a resolution of 500 m. ICESat-2 only reaches a DEM resolution of 700 m at the equator but increases to almost 200 m at higher latitudes. When combined, a 500 m resolution lidar-based DEM can be achieved globally. Our results indicate that both ICESat-2 and GEDI enable accurate terrain measurements anywhere in the world. Especially in data-poor areas—such as the tropics—this has potential for new applications and insights.

Keywords: ICESat-2 ATL03, GEDI L2A, DTM, lidar, altimetry, validation, laser, terrain, vertical accuracy, spatial coverage, global

1. Introduction

Digital Elevation Models (DEMs) greatly impact the confidence in modelling many large-scale environmental processes. In this respect, airborne lidar has had a large impact, and for larger areas, space technology has also been playing an important role. Yang et al. (2011) give a detailed overview of the advances that DEMs from space can offer for applications in various fields, such as the detection of geological structures (Masoud and Koike, 2011), the analysis of tectonic evolution (Meigs, 2013), the understanding of volcanic processes (Funning et al., 2005), and assessing flood vulnerability (Hooijer and Vernimmen, 2021;

*Corresponding author
Email addresses: maarten.pronk@deltares.nl (Maarten Pronk), h.ledoux@tudelft.nl (Hugo Ledoux), marieke.eleveld@deltares.nl (Marieke Eleveld)

Schumann and Bates, 2018). However, as pointed out by Schumann and Bates (2018), current *global* DEMs are often less suitable as input for those tasks than DTMs acquired with airborne lidar. Compared to airborne lidar DTMs (Mallet and Bretar, 2009), (1) they have larger vertical errors, (2) their resolution is low, and (3) often they represent the Digital Surface Model (DSM) (vegetation and man-made structures are present) of an area instead of the terrain. These inherent issues stem from the primary measurement methods used in constructing the global DEMs—either interferometry using C-band and X-band radar (SRTM, Tandem-X) or stereoscopy using passive optical imagery (ASTER, ALOS)—to measure elevation (Moudry et al., 2018); whereas lidar can penetrate canopy.

In this study, we aim to investigate the application of spaceborne lidar altimetry data as an alternative to interferometry/stereoscopy to model global DEMs. Specifically, we investigate data from two missions: (1) ICESat-2, which is in a polar orbit to investigate ice sheets (Markus et al., 2017; Neuenschwander and Pitts, 2019) as its primary objective, but it also measures canopy height (Neuenschwander and Pitts, 2019) among others; and (2) GEDI, which is attached to the ISS and whose primary goal is to investigate global ecosystems (Schneider et al., 2020; Dubayah et al., 2020). While these two missions have primary objectives other than terrain modelling, it is possible to also use and combine them for modelling terrains.

For instance, for ICESat-2, Neuenschwander et al. (2020) report a 0.53 m Mean Absolute Error (MAE) and 0.73 m Root Mean Square Error (RMSE) when carefully validating 193 ICESat-2 satellite overpasses in Finland, Malambo and Popescu (2021) report a MAE of 1.20 m for different biomes in the USA, and Wang et al. (2019) report a RMSE of 1.96 m for terrain heights from unclassified ICESat-2 ATL03 product by applying the noise filter proposed by (Zhu et al., 2018). As for GEDI, it has been used less for terrain applications. A validation study with reference areas in Germany by Adam et al. (2020), using the GEDI L2A product (version 1), shows a Median Absolute Deviation (MAD) of 3.42 m, but it should be noted that 2 out of 19 orbits included showed a significant increase in error metrics that they could not account for. Quiros et al. (2021) found a 6.05 m RMSE for terrain heights of the GEDI (L2A, version 1) product in southwest Spain. They also found that by—accounting for the geolocation error—moving the footprints 10 m to the west the results were improved. Zhao et al. (2022) reported a horizontal geolocation error of 1.7 m for ICESat-2. Liu et al. (2021) were the first to combine both GEDI (L2A, version 2) and ICESat-2 (ATL08, version 4) in a validation study of 7000 km^2, finding RMSEs of 4.03 m and 2.24 m, respectively. More recently, Urbazaev et al. (2022) also combined GEDI (L2A, version 2) and ICESat-2 (ATL08, version 5) in a large validation study, finding a bias of less than a metre for both datasets. Lastly, Zhu et al. (2023) determined terrain accuracy underneath short-stature vegetation for several study sites in the USA, finding a bias of -0.05 m for ICESat-2 and a bias of 0.39 m for GEDI. Because of their good vertical accuracy, GEDI and ICESat-2 can be used to correct global DEMs, see for instance (Magruder et al., 2021; Hengl et al., 2020; Okolie and Smit, 2022; Pronk et al., 2024).

To reconstruct a terrain from altimetry observations, more than a good vertical accuracy is required: a adequate density of observations on the surface of the Earth is also necessary to obtain good results from spatial interpolation and this aspect has received less attention. As can be seen in Figure 1, both satellites reach their highest density of ground tracks at their inclination angle, but are least dense on the equator. ICESat-2—planned to have a 2 km maximum track seperation (Markus et al., 2017)—has been used to generate coarse resolution terrain models, one for Antarctica (Shen et al., 2021) covering 72% of the 1 km grid and a global lowland terrain model at ∼1 km (Vernimmen and Hooijer, 2023). GEDI has not yet been used for the generation of global DEMs, neither on its own nor in combination with ICESat-2. In the future, both the ICESat-2 and GEDI teams plan to produce 1 km, or coarser, raster products (respectively for level 3 and level 3B (ATL18)). For example, the GEDI team has already published the 1 km resolution L3 Gridded Land Surface Metrics product (Dubayah et al., 2021b), but not all cells are filled. Notably, these resolutions are an order of magnitude lower than the along-track resolution of ICESat-2 or GEDI. The *possible* resolution of a global DEM based on ICESat-2 and/or GEDI data has not yet been studied.

In this study, we assess whether, and to what extent, the measurements from ICESat-2 and GEDI—based on their vertical accuracy and spatial coverage—can be used as a basis to reconstruct global DEMs. We validate the altimetric measurements of both missions by comparing them against airborne lidar measurements of three locations representing different terrain types (the Netherlands, Switzerland, and New Zealand). To our knowledge, by using all ICESat-2 and GEDI data at their latest version—and reference

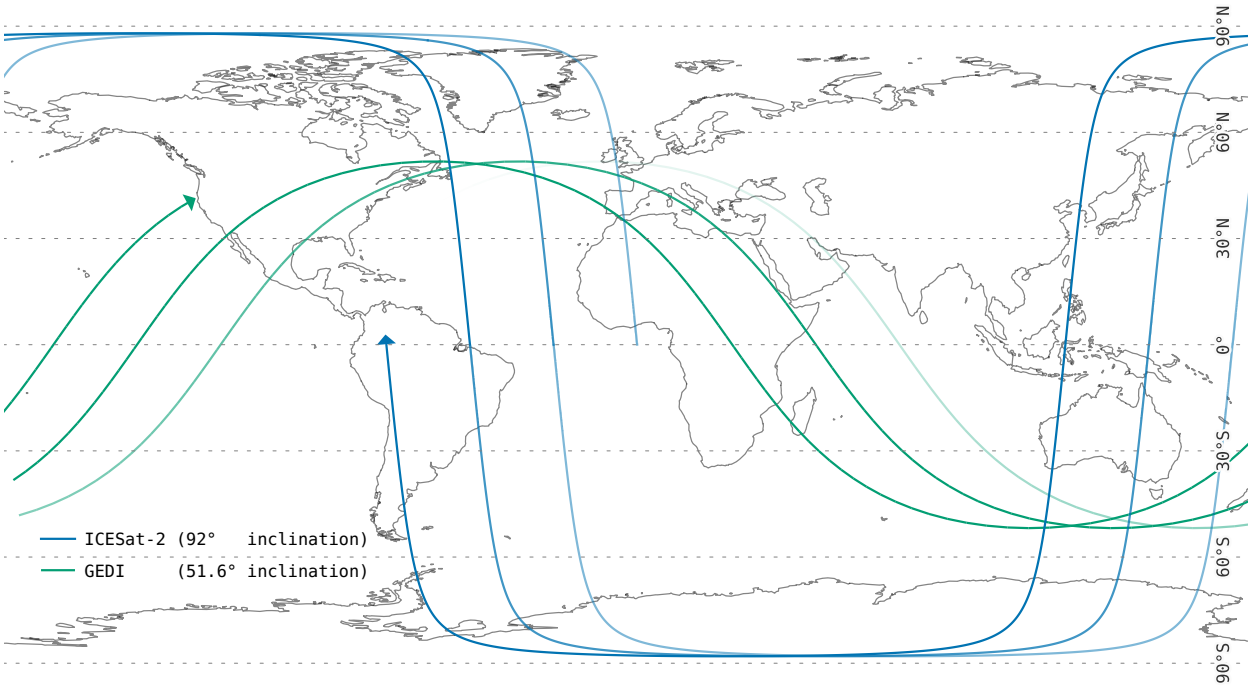

Figure 1: Ground tracks for three successive orbits of ICESat-2 and GEDI. The satellite is represented by a triangle and past orbits fade out. Note the increased density of ground tracks at the latitude of inclination, as well as the lack of coverage beyond 51.6° latitude for GEDI.

data from several countries—we present the most representative and extensive validation study (using over 225 million samples) for these datasets thus far. Unlike previous studies, we use the lowest possible level of the products (we do not use aggregates or gridded samples). Furthermore, unlike previous studies, we assess the density of samples in the planimetric direction for large areas ranging from the equator to the poles, which allows us to identify which resolutions of a (global) DEM could be achieved. Also, we consider and study other factors that can influence the quality of the altimetric measurements—and thus serve as possible filters—strong/weak beams, day/nighttime, terrain slope, seasonal effects, outlier tracks and the presence of water. Our final results should then allow practitioners used to airborne lidar to make informed decisions, such as choosing to filter certain ground tracks that contain mostly outliers.

2. Datasets & Methods

2.1. ICESat-2 and GEDI

The Low-Earth Orbit (LEO) of ICESat-2 at an orbit inclination of 92°, covers the earth between −88° and 88° latitude. The laser of its instrument (ATLAS) splits into six beams, divided into three pairs, each pair 90 m apart and the pairs 3.3 km apart, for a total swath width of 6.6 km. Each pair contains a strong beam (pulse energy of 120 μJ) and a weak beam (pulse energy of 30 μJ), with a power ratio of 4:1 (Markus et al., 2017; Magruder et al., 2024). Along-track, it can measure every 0.7 m, while its beam footprint is ∼11 m, consecutive measurements thus overlap.

The orbit of GEDI, itself attached to the Japanese Experiment Module at the International Space Station (ISS), is between 51.6° N and 51.6° S. Its three lasers split into eight beams, each 600 m apart, for a total swath width of 4.2 km. Of the eight beams, four are strong (pulse energy of 15 000 μJ) while the other four are weak beams (pulse energy of 4500 μJ), with a power ratio of 3.3:1 (Wake et al., 2019; Dubayah et al., 2020). GEDI measures a point every 70 m along-track, with a beam footprint of 23 m.

Table 1: Key characteristics of GEDI and ICESat-2 missions in comparison with a typical airborne mission.

Mission	ICESat-2	GEDI	Airborne lidar
Type	Discrete photon	Full waveform	Either
Main objective	Cryosphere monitoring	Ecosystems	-
Duration	2018–now (ongoing)	2019–2023 (2024-)	Single flight(s)
Orbit Inclination	92°	51.6°	NA
Laser pulse power	1x 660 μJ	3x 10 500 μJ	200 μJ to 8000 μJ
Beam power (strong/weak)	120 μJ/30 μJ	15 000 μJ/4500 μJ	200 μJ to 8000 μJ
# tracks	6 (in 3 strong/weak pairs)	8 (four strong, four weak)	1
Altitude	∼480 km	∼420 km	0.5 km
Track footprint	11 m	23 m	0.05 m
Along track spacing	0.7 m	70 m	0.1 m
Across track spacing	3 km/90 m between pair	0.6 km	0.1 m
Swath width	6.6 km	4.2 km	1 km
Beam frequency	532 nm (green)	1064 nm (near-infrared)	Either

Both missions have multiple laser beams and a division in beam energy, resulting in weak and strong beams. Weak beams (or coverage beams) are a way to improve coverage while still maintaining the mission requirement(s) for a specific power level with the strong beams. Coverage is further increased for both missions by the ability to angle the instruments away from their reference ground tracks (Neuenschwander and Pitts, 2019; Dubayah et al., 2020), preventing repetitions of the same ground track. The characteristics of both missions are summarised in Table 1.

The data from the ICESat-2 and GEDI missions are made publicly available in several data products, categorised in subsequent Level 1, 2, and 3 data products. Level 1 products contain the raw telemetry, whereas Level 2 products contain directly usable geolocated data to which several corrections—such as accounting for atmospheric effects—are applied. Data for Level 3 are aggregated versions of Level 2 products, which are smaller in filesize and easier to process. ICESat-2 differentiates between a Level 3A, which aggregates consecutive samples along the ground track of Level 2 data products, and a Level 3B, which are gridded versions of the aggregated Level 3A data products. GEDI's Level 3 data products are gridded versions of Level 2 data products, like ICESat-2's Level 3B.

Both missions make their data available online in *granules*, which are subsections of a single orbit. GEDI divides one orbit into 4 granules (but only since version 2), while ICESat-2 has 15 granules per orbit. The Land Processes (LP) Distributed Active Archive Center (DAAC) distributes the GEDI L2A data, while the National Snow and Ice Data Center (NSIDC) DAAC distributes ICESat-2 data.

We used the ICESat-2 Level 2 ATL03 product (Neumann et al., 2021), currently at version 6, with dates ranging from 2018-10-13 to 2023-10-26. This dataset is not classified, so we used the classification *signal_photons/classed_pc_flag*, which is a flag from the higher Level 3 ATL08 product (Neuenschwander et al., 2021) to classify each photon. These classifications include "noise", "ground", "canopy" and "top of canopy", of which we only use "ground". For elevation, we used the *heights/h_ph* (height photon) containing the elevation above the WGS84 ellipsoid and related latitude *heights/lat_ph* and longitude *heights/lon_ph* for each track group in the HDF5 file. We did not apply further filtering but noted that classified points have a confidence level of 3 (medium) or 4 (high) by design, thereby filtering out lower confidence values.

To investigate the performance of GEDI, we used the GEDI L2A data product (Dubayah et al., 2020, 2021a) at version 2. As of writing, this covers dates from 2019-04-18 to 2023-07-16. For elevation, we used the *elev_lowestmode* field and related latitude *lat_lowestmode* and longitude *lon_lowestmode* fields for each track group in the HDF5 file. We filtered the data based on the settings that are used to produce the higher level L3A (version 2) product (Dubayah et al., 2021c), which uses points from the L2A product in a sparse 1 km resolution raster product. These settings only include data with the flags *rx_assess_quality_flag* set to non-zero, *surface_flag* set to non-zero and *degrade_flag* set to zero, with all flags specified in Appendix A.

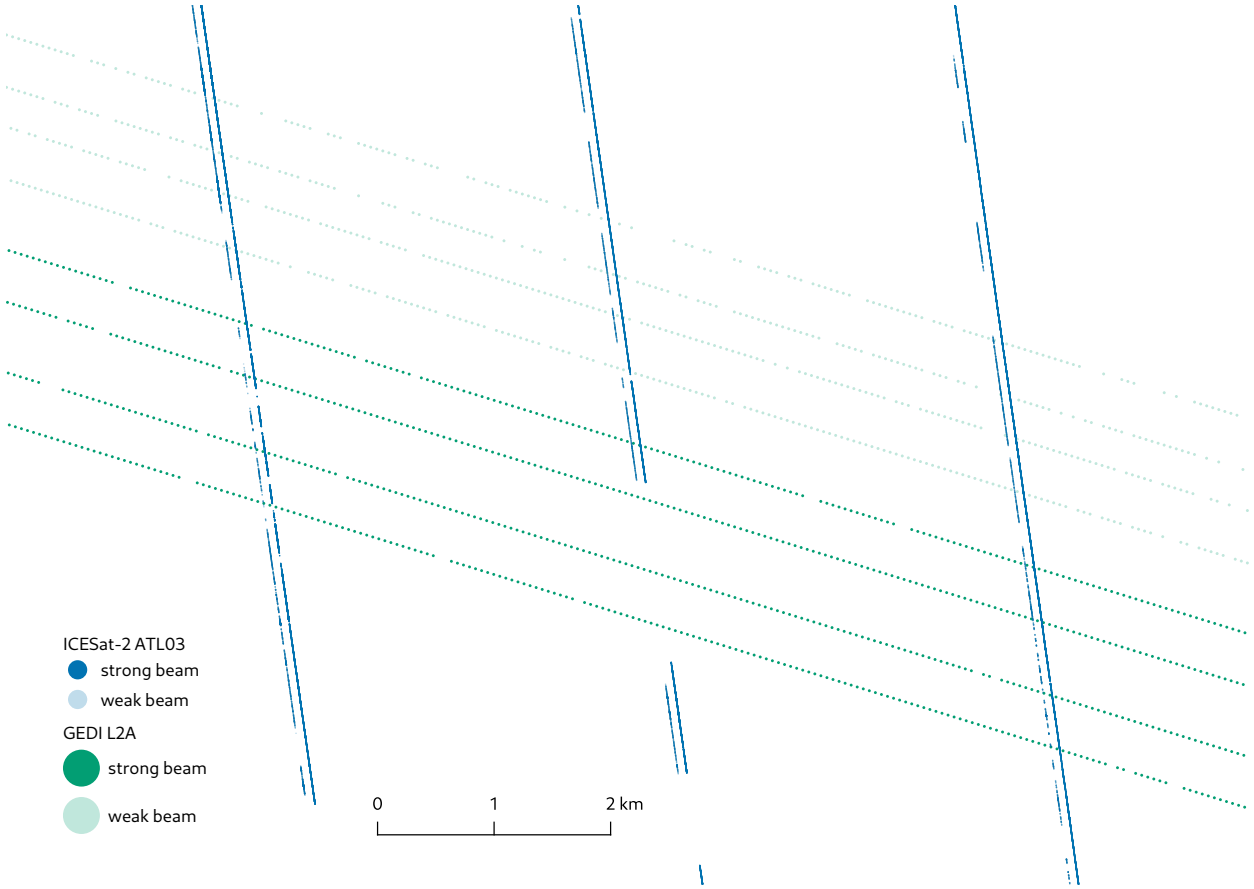

Figure 2: Filtered ICESat-2 ATL03 (blue) and GEDI L2A (green) points from a single granule each at the 47th latitude to scale, demonstrating the beam patterns. Note that ICESat-2 has a smaller beam footprint and a much higher pulse repetition, but a more uneven spatial coverage than GEDI. The gaps between data here will decrease by using multiple granules, but will never disappear completely.

2.2. Reference datasets: airborne lidar and land cover

We compared ground elevation points from both missions with terrain reference datasets based on airborne lidar. Areas included are the Netherlands, Switzerland, and New Zealand, for a total of 25 663 km^2. These datasets cover flat to steep terrain and several forest types in different climate zones of the world. Note that GEDI doesn't cover the full area of the Netherlands, as it orbit terminates at 51.6° latitude.

The validation dataset used for the Netherlands is the 5 m DTM version of the AHN4 (2020–2021), sourced from `https://www.ahn.nl/ahn-viewer`. Referencing to the ellipsoid was conducted with the pipeline described with RDNAPTRANS2018, requested from `https://www.nsgi.nl/geodetische-infrastructuur/coordinatentransformatie`. The validation dataset used for Switzerland is the 0.5 m DTM version of the Kanton Zürich (2017–2018) dataset based on swissSURFACE3D, sourced from the Geographisches Informationssystem des Kantons Zürich (GIS-ZH), the Digitales Terrainmodell (DTM) `https://geolion.zh.ch/geodatensatz/3508`. Referencing to the ellipsoid was conducted by the geoids provided at `https://cms.geo.admin.ch/ogd/geodesy/Geoid_OGD.zip`. The validation dataset used for New Zealand is the 1 m DTM version of the Auckland South lidar (2016–2017) dataset, sourced from the LINZ Data Service (`https://data.linz.govt.nz/`) and licensed for reuse under CC BY 4.0. Referencing to the ellipsoid was conducted by the geoids provided at `https://www.geodesy.linz.govt.nz/download/proj-datumgrid-nz`. An overview is given in Table 2.

Note that airborne lidar datasets differ considerably from spaceborne lidar, most notably so in their

Table 2: Reference datasets based on airborne lidar with the amount of ICESat-2 and GEDI granules that intersect each area.

Country	the Netherlands	Switzerland	New Zealand
Latitude	50°-53°N	47°N	37°S
Dataset	AHN4	Kanton Zürich	Auckland South
Years collected	2020-2021	2017-2018	2016-2017
Area	21 800 km^2	1728 km^2	2135 km^2
Resolution	5 m	0.5 m	1 m
Uncertainty	<0.1 m	<0.1 m	<0.1 m
Terrain type	Delta	Mountainous	Foothills
Elevation range	0-300 m	350-1300 m	0-700 m
ICESat-2 granules	680	146	147
ICESat-2 size	1072 GB	270 GB	118 GB
GEDI granules	2029	268	196
GEDI size	3791 GB	543 GB	232 GB

platform, resulting in considerable differences in beam footprint and ground coverage (see Table 1). The altitude increase results in a wider beam footprint, from ∼0.5 m (at 500 m (van Dijk and Bos, 2013)) for airborne platforms to ∼20 m for space platforms. Although much wider, it is a small increase compared to the increase in sensing altitude, going from 0.5 km to 480 km. Airborne lidar often focuses on maximising coverage (points/m^2) of smaller areas, whereas the coverage for space lasers is the ground track of the satellite. While both ICESat-2 and GEDI employ instruments with multiple (split) laser beams, including the ability to point the laser away from the ground track—all to maximize coverage—this still results in very sparse and uneven coverage as shown in Figure 2. A comparison is given in Table 1.

In order to differentiate the results from the comparison with the reference datasets, we also sampled the land cover class from the ESA WorldCover 2020 dataset (Zanaga et al., 2021). WorldCover recognizes several land cover classes, such as “Grassland”, “Cropland”, “Tree cover” and “Built-up”, that we used to differentiate the error metrics.

An overview of these datasets for the area of New Zealand is given in Figure 3. The overviews for the two other reference areas are in Appendix B.

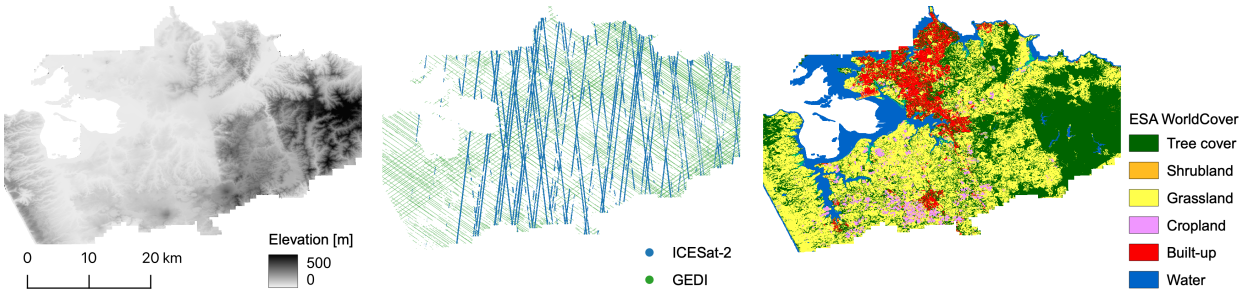

Figure 3: A visual overview of the datasets used for the reference area in New Zealand. On the left is the airborne lidar DTM, in the middle the spaceborne lidar data, and on the right the landcover classes according to ESA WorldCover.

2.3. Methods

This study investigates the vertical accuracy of both ICESat-2 ATL03 and GEDI L2A data by comparing them with DTMs based on airborne lidar in different countries and terrain types. Furthermore, we assess the density of samples in the planimetric direction to identify which resolutions of a (global) DEM based on

ICESat-2 and/or GEDI could be achieved. The ATL03 and L2A products, both Level 2 products, are the lowest level or highest resolution data products available for both missions that are geolocated and corrected for geophysical effects, thus containing directly applicable elevation values. We differ from most studies in using the Level 2 ATL03 data product for ICESat-2, and not its Level 3 ATL08 product, which is a 100 m aggregated version of ATL03.

All granules intersecting with the reference areas were searched using NASA Earthdata Search and downloaded from their archive centres. This download resulted in 3466 granules with a total size of ∼5.9 TB, as detailed in Table 2. After data filtering—for both quality and geographic area—data from a remaining 1941 granules (56%) were used.

For each ICESat-2 or GEDI measurement z, we retrieved the corresponding cell values from the reference raster datasets. Given a 5 m resolution reference raster, ICESat-2—with a 11 m footprint—covers roughly 2×2 cells. GEDI, with its slightly larger footprint, would cover 5×5 cells. Our experiments showed there is no discernable difference between sampling the centre cell, the mean or median of all cells. We take the centre cell—the midpoint of the beam—to obtain a single value c which we use in the following metrics:

$$\text{Mean Error (bias)} = \frac{1}{n}\sum_{i=1}^{n}(z_i - c_i) \tag{1}$$

$$\text{Mean Absolute Error (MAE)} = \frac{1}{n}\sum_{i=1}^{n}|z_i - c_i| \tag{2}$$

$$\text{Root Mean Square Error (RMSE)} = \sqrt{\frac{1}{n}\sum_{i=1}^{n}(z_i - c_i)^2} \tag{3}$$

In order to assess the coverage of ICESat-2 and GEDI—and thus the possible resolution of a (global) DEM based on ICESat-2 and GEDI lidar—we rasterised ICESat-2 and GEDI data into 5 km x 50 km rasters at several resolutions for a full range of latitudes. We did so along the 99th meridian east, as it is one of the few areas which has almost continuous landmass from the 0° latitude northward. Similar to the procedure followed in assessing the vertical accuracy, all granules intersecting with a meta-bounding box around the 99th meridian east were downloaded and processed. This download resulted in 2715 ICESat-2 granules and 8760 granules for GEDI, over 20 TB of data.

The raster values were obtained by counting the samples (footprints) falling inside each raster cell. Rasterising at a high resolution will thus leave many cells empty (set to 0), while rasterising at a low resolution will fill up the entire grid with values equal to or larger than one. We denote the ratio of non-zero cells over all raster cells in a 5 km x 50 km box as the *spatial coverage (%)*. At 100%, it gives a lower bound to the density: at least 1 point per cell at a given resolution. An example for a grid with a 100 m resolution is given in Figure 4. Given the possible presence of waterbodies—and thus gaps in the coverage—a 100% spatial coverage is unrealistic. Here, we qualify spatial coverages of 80% and up fit for DEM creation purposes.

An overview of the methodology is given in Figure 5. The above-mentioned search, extraction, sampling and rasterisation algorithms have been implemented in the programming language Julia (Bezanson et al., 2017). The code—making use of the the open-source package SpaceLiDAR.jl (Pronk and Gardner, 2021)—and instructions are available at `https://anonymous.4open.science/r/icesat2-gedi-val-dtm`.

3. Results

3.1. Accuracy

When compared with the airborne DTMs across all three validation areas, ICESat-2 achieves a bias of −0.11 m, a MAE of 0.43 m, and a RMSE of 0.93 m (N=236 932 686). GEDI is less accurate with a bias of 0.09 m, a MAE of 0.98 m, and a RMSE of 2.96 m (N=15 544 899) as demonstrated in Table 3. In this

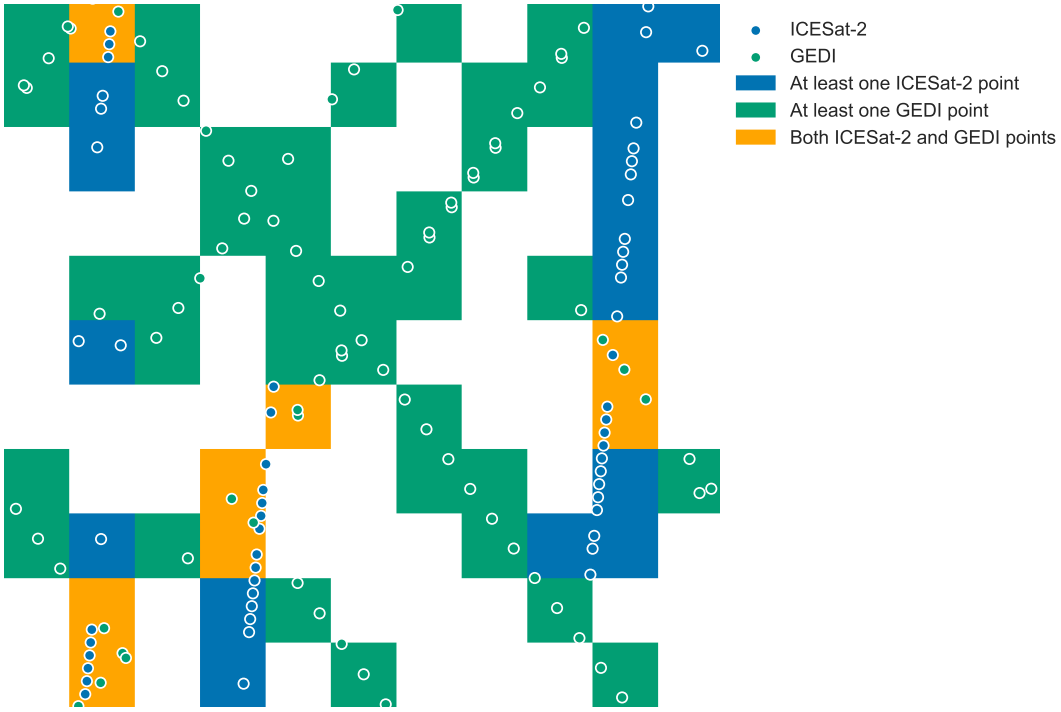

Figure 4: A 11 × 11 100 m resolution grid with ICESat-2 and GEDI footprint centres rasterized. Cells without points—59 out of of 121 or 49 %—are white. Together, ICESat-2 and GEDI fill 62 out of 121 cells, a *spatial coverage* of 51 %.

comparison, ICESat-2 has ∼15 times more samples than GEDI, which is less than the expected factor of hundred from their along track spacing specifications. The imbalance in the number of samples skews the accuracy in favour of ICESat-2 when all samples are combined, resulting in a bias of −0.12 m, a MAE of 0.47 m, and a RMSE of 1.17 m (N=252 477 585).

Open land cover, such as "Cropland" and "Grassland", result in the best precision for both missions. Precision decreases in "Sparse vegetation" areas and is worst in "Tree Cover" for GEDI and in "Built-up" areas for ICESat-2. Both missions are the least accurate in urban areas, as they mistake buildings for ground, resulting in a strong positive bias of half a metre (0.65 m bias for ICESat-2, 0.47 m bias for GEDI).

In terms of accuracy, ICESat-2 exhibits a small negative bias (which is partially obfuscated by the positive bias in "Built-up" areas). Conversely, GEDI has a positive bias, mostly due to the "Tree cover" and "Built-up" areas. These biases are present and consistent in all validation areas. Separate results for each validation area are provided in Appendix C.

There is a considerable tail present in the distribution of these differences, which is to be expected based on the total number of measurements. In Figure 6, we show the elevation differences with the reference dataset from Table 3. We used so-called boxenplots or letter-value plots to also visualize the (shape of the) tail of these large datasets (Hofmann et al., 2017). Note that ICESat-2 has more negative than positive outliers (a negative skew), while the outliers of GEDI are balanced (zero skew), except in "Built-up" areas.

3.2. Spatial coverage

Figure 7 shows which percentage of cells within a grid intersect with ICESat-2 and GEDI data for multiple resolutions and latitudes on the 99th meridian east. Note that coverage is low over oceans, lakes, and rivers, and that our ATL03 classification with ATL08 excludes polar ice. Near the poles, it is possible to achieve a 200 m resolution with ICESat-2 as roughly 86 % of the cells are filled with at least one data

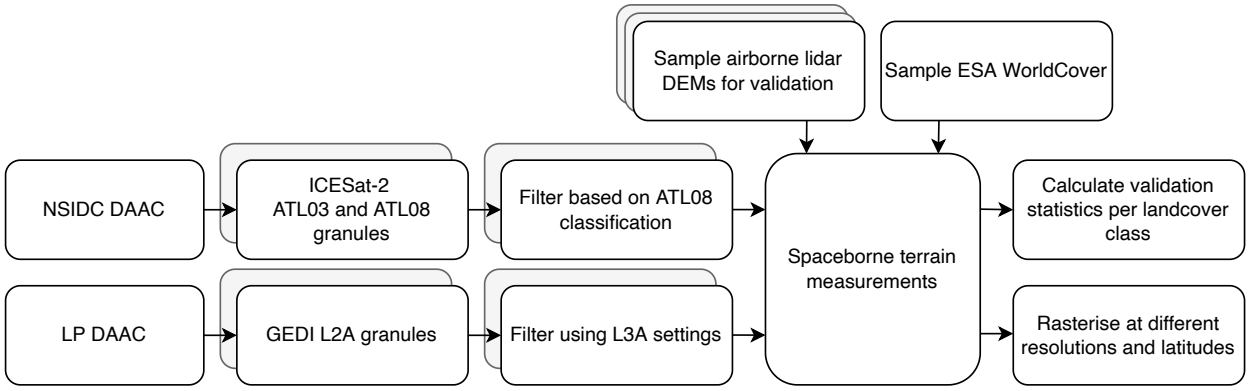

Figure 5: Overview of the datasets and methods used in this study.

Table 3: Validation of ICESat-2 ATL03 and GEDI L2A terrain data with reference areas for each landcover class. n is the number of observations.

Landcover	bias [m]		MAE [m]		RMSE [m]		n	
	ICESat-2	GEDI	ICESat-2	GEDI	ICESat-2	GEDI	ICESat-2	GEDI
Tree cover	−0.26	0.36	0.55	1.67	1.08	4.64	28 435 933	3 967 497
Built-up	0.64	0.47	1.17	1.13	2.31	2.64	16 849 903	1 086 164
Grassland	−0.18	−0.08	0.38	0.79	0.7	2.33	129 362 404	6 043 868
Bare / sparse vegetation	−0.19	−0.09	0.47	1.17	1.23	3.56	3 360 391	133 912
Cropland	−0.09	0.01	0.27	0.57	0.5	1.45	50 267 300	4 186 557
Herbaceous wetland	−0.23	−0.03	0.31	0.56	0.59	0.97	8 656 755	126 901
All landcovers	−0.11	0.09	0.43	0.98	0.93	2.96	236 932 686	15 544 899

point. Moving towards the equator, with the addition of GEDI from the 51st latitude onwards, the combined achievable resolution is 500 m.

GEDI achieves a more even sampling density due to the configuration of the ICESat-2 beam pairs in combination with the high inclination (see Figure 2). Indeed, GEDI consistently fills more raster cells than ICESat-2 in Figure 7, reaching a possible 700 m resolution around the equator on its own, whereas ICESat-2 only reaches 1000 m.

3.2.1. Influence of strong and weak beams

Both ICESat-2 and GEDI have strong and weak beams, and weaker beams are not expected to fully penetrate dense canopy. However, after data filtering, the accuracy for both the strong and weak beams is comparable for both missions, as shown in Figure 8a. The weak beam measurements are only slightly less accurate than those from the strong beam. To achieve this accuracy, we note that the weak beam data only accounts for 20% of the ICESat-2 data, the rest of the data has been filtered out. This effect was already visible in Figure 2. Remarkably, GEDI has a much higher percentage of weak beam data (roughly 50%) and still achieves comparable accuracy to its strong beam. We suspect that this can be explained by the much higher pulse energy of the full-waveform lidar instrument of GEDI compared to single-photon lidar of ICESat-2, combined with the lack of dense (tropical) canopy in our validation areas.

3.2.2. Solar background influence

Lidar instruments, especially those with wavelengths like ICESat-2's green 532 nm, but also GEDI's near-infrared 1064 nm one, are potentially sensitive to background noise from the sun (Neumann et al., 2019; Dubayah et al., 2020), as their spectra overlap (Thuillier et al., 2003). In both cases an additional

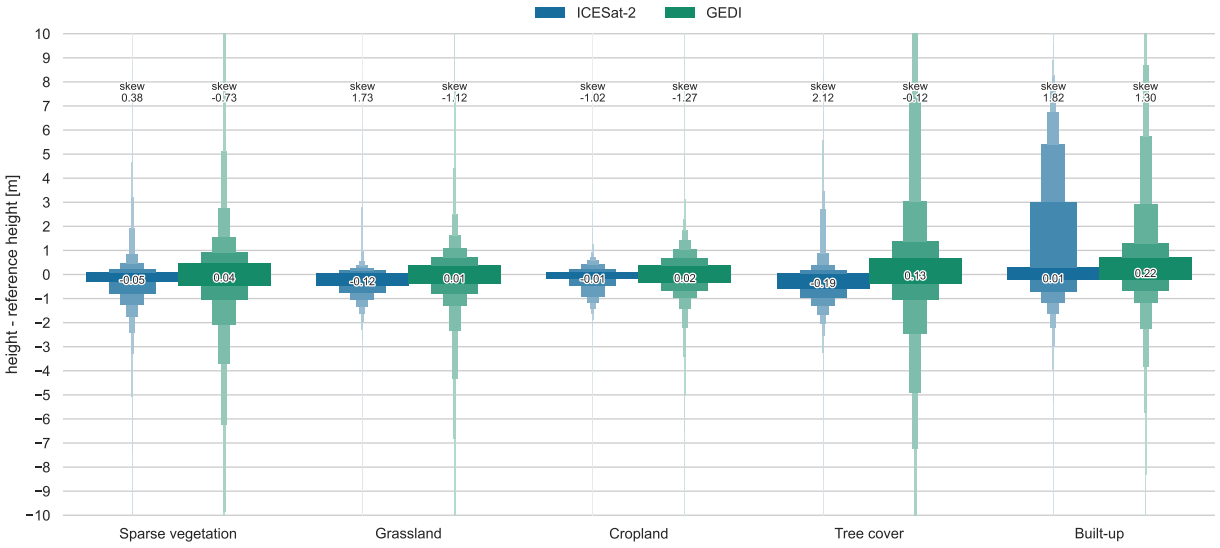

Figure 6: Elevation difference as boxenplots for both missions compared to reference areas per landcover type (ESA Worldcover). The median (centre) and skewness (top) is also given for each boxenplot. ICESat-2 is more accurate (MAE 0.43 m, bias of −0.11 m) as GEDI (MAE 0.98 m, bias of 0.09 m). GEDI performs worst in "Tree cover" areas, while ICESat-2 performs the worst in "Built-up" areas.

radiance signal from sunlight will be scattered into the telescope from atmosphere and surface. Single-photon lidar instruments like ICESat-2's ATLAS are potentially more sensitive to this effect than the stronger full-waveform lidar of GEDI. It is expected that measurements made during the day are less accurate than those done during the night. However, as seen in Figure 8b, the results are comparable between daytime and nighttime. We do note however that slightly more data is filtered out for both ICESat-2 and GEDI during the day.

3.2.3. Seasonal influence

In the parts of the world with leaf-on and leaf-off seasons, airborne lidar is often collected during winter to maximize ground returns, as there is less canopy to reflect on. Indeed, the airborne lidar reference datasets from the Netherlands and Switzerland have been collected in winter. However—while there are differences between different months—we find no clear seasonal pattern when the measurements are split for each month of the year (Figure 9), even when only taking measurements within the "Tree cover" class of the WorldCover land cover classification into account.

3.2.4. Geolocation accuracy

Depending on the slope of the terrain, horizontal geolocation errors can result in considerable vertical errors. Indeed, slope is one of the major factors influencing the accuracy of lidar (Su and Bork, 2006). This is especially true for spaceborne lidar with much larger geolocation errors and footprints than airborne lidar: a measurement at the edge of ICESat-2's 11 m footprint on a slope of 25 % will result in a vertical error of 1.4 m compared to a centre measurement.

In Figure 10 we plot the difference between ICESat-2 and GEDI and the reference for different slopes in Switzerland. We observe a clear decrease in both accuracy as precision with slope, and note that for both missions the bias is negatively correlated. ICESat-2's accuracy suffers less from slope than GEDI, but both are directly related to their geolocation accuracy. For steeper slopes, little to no skewness is observed. ICESat-2 has a positive skewness on 0° to 10° slopes, due to the presence of urban areas.

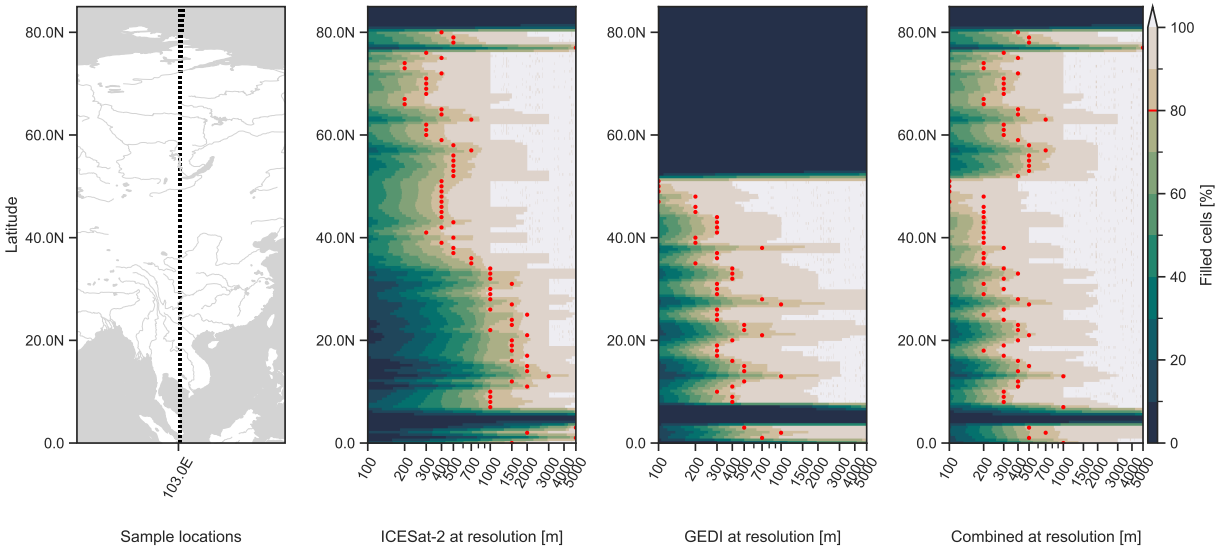

Figure 7: Spatial coverage (% of cells filled) for several grid resolutions at each latitude. Red points for 80 % spatial coverage is also given. By combining both ICESat-2 and GEDI a 500 m (with >80% filled) resolution DEM is possible. Note that locations over oceans, lakes and rivers have a low coverage. The sample locations (5*10 km rasters as black rectangles) appear wider at higher latitudes due to the map projection.

3.2.5. Presence of water

The presence of water can result in specular reflections. When combined with the previously discussed overlapping laser footprint for ICESat-2 (with the reported location being the centroid of the footprint), the presence of water at the edge of the footprint can thus become the dominant elevation signal. In effect, this widens water bodies with half of the footprint, which is significant (7 m to 8 m) for smaller water bodies such as streams. This phenomenon shows up as negative outliers near (the edge) of water, as shown in Figure 11a. As GEDI has a larger footprint, it is theoretically more prone to this effect than ICESat-2, but the footprints do not overlap (every 70 m for GEDI), and we have not observed this effect in the data.

4. Discussion

4.1. Factors influencing the accuracy

Well-calibrated and validated ICESat-2 and GEDI mission product versions have become available, here we have used the latest version 6 of ICESat-2 ATL03 and version 2 of GEDI L2A. Our results for both ICESat-2 and GEDI are comparable to findings from previous studies—even though the study areas differ. Wang et al. (2019) reported a RMSE of 1.96 m for terrain heights from the unclassified ICESat-2 ATL03 product, compared to our 0.93 m. A better RMSE of 0.75 m was reported by Xing et al. (2020), but with only two beams of single granule their number of samples was limited. The 2.96 m RMSE for GEDI found here is better than the 6.05 m RMSE found by Quiros et al. (2021) in southwest Spain. Similarly, Liu et al. (2021) found a worse RMSE of 4.03 m for GEDI than ours, and a worse MAE of 1.80 m (ours 0.98 m) and bias of 0.97 m (ours 0.09 m). We suspect our GEDI data (collected during 2019–2023) contains less outliers due to a different distribution of landcover classes than the data used by Liu et al. (2021) (collected during 2019, with no differentiation per landcover class), which explains the difference in RMSE. Like Urbazaev et al. (2022) and Zhu et al. (2023) we found that ICESat-2 and GEDI both have sub-meter biases. These biases can be measured in centimetres, approaching airborne lidar territory.

All reference datasets are based on lidar and have accuracies within ∼10 cm. These datasets were collected between 2020–2021 (the Netherlands), 2017–2018 (Switzerland) and 2016–2017 (New Zealand),

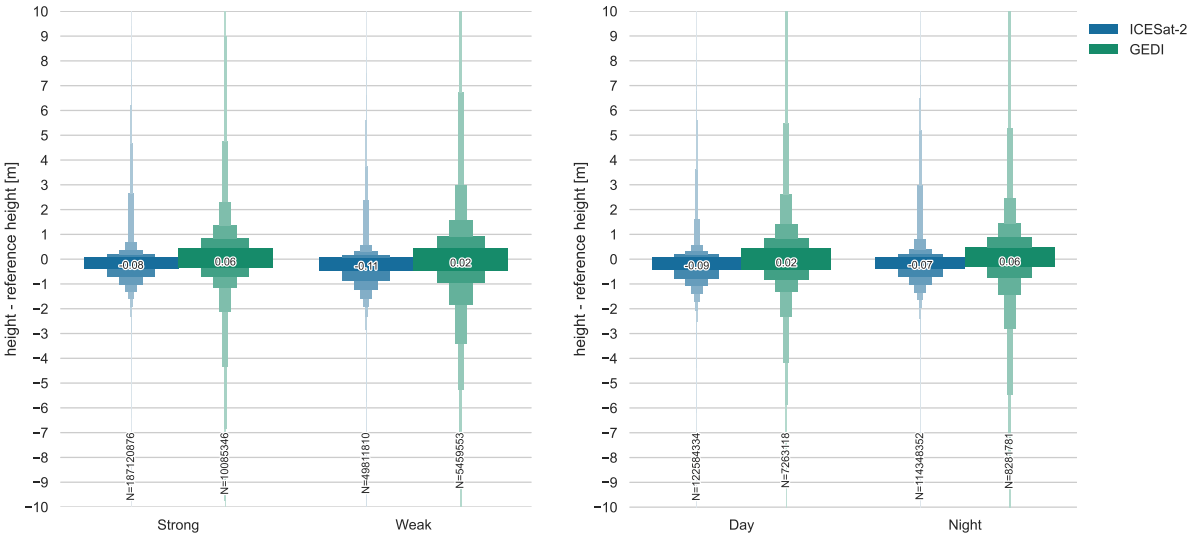

Figure 8: Terrain elevation difference for both missions compared to reference by (a) beam power and (b) time of day. The median, and the number of samples is included in the middle and lower part of the figure, respectively. Overall the results are similar for both comparisons and missions, but note that ICESat-2 filtered much more data from its weak beam than GEDI.

while ICESat-2 data are from 2018–2022 and GEDI data are from 2019–2022. Some inaccuracies found here—mostly for the urban areas—could thus stem from temporal differences.

4.1.1. Geolocation accuracy

Neuenschwander and Magruder (2019) found an increase in vertical accuracy by horizontally offsetting the location by −5 m along track, thereby accounting for possible geolocation errors. We repeat our accuracy measurements in the Swiss reference area—the one with the most relief—with several offsets based on the movement direction of the satellite. The offsets are specified as 2.5 m, 5 m, and 10 m in forward, backward (along-track) and left, right (across-track) directions. However, we find no consistent improvement in accuracy for any of the offsets. For limited selections of steeper slopes, we do find bias improvements by using offsets, but note that these are likely due to a small number of samples in specific terrain. We thus could not replicate the findings of Neuenschwander and Magruder (2019), nor those of Quiros et al. (2021), who found that accuracy for GEDI increased by offsetting the location 10 m to the left. However, we respectively use the version 5 of ICESat-2 ATL03 and version 2 of GEDI L2A in our study (versus version 1—both for ICESat-2 and GEDI—in theirs). GEDI version 2 has significantly improved the geolocation error (Dubayah et al., 2021a), which we confirm here.

4.1.2. Outlier tracks

We note that several granules of both ICESat-2 and GEDI missions contain consistent gross outliers. The elevations provided in these granules are consistently much higher or lower than the reference elevation, often tens of meters. This was previously reported for GEDI by Adam et al. (2020). For some tracks, a timing error related to satellite orbit is the most likely source of these outliers, as all elevations are offset by roughly the same error, and the profile of the terrain is visible. In other cases, cloud cover impact—for example above valleys in mountainous terrain—is the most likely source of these outliers. For ICESat-2 a list of retracted granules was published for version 3 of the data, which have been fixed in subsequent versions. For GEDI no such list exists as of writing, although one is mentioned in the GEDI documentation for Level 3 products.

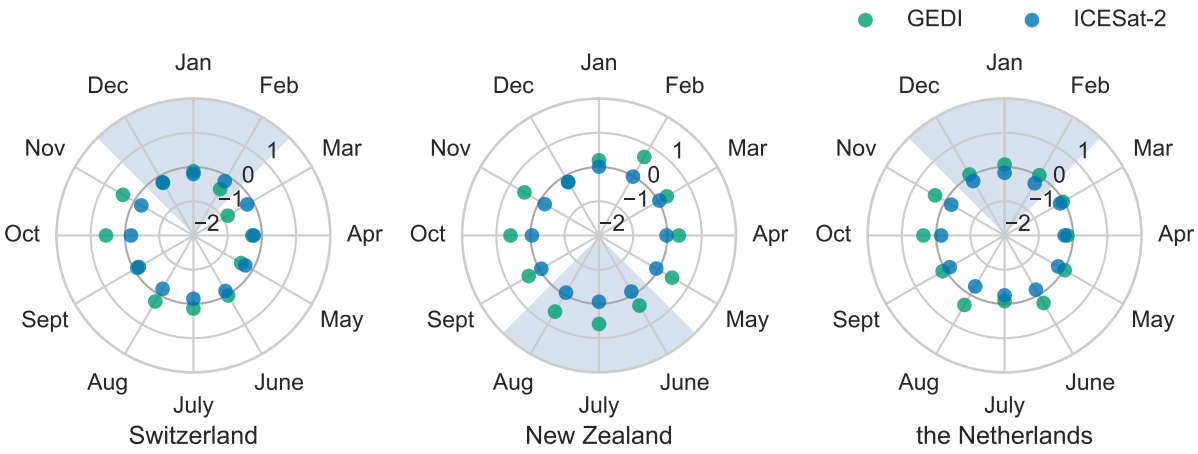

Figure 9: The bias of ICESat-2 and GEDI split out per month and reference area in rose plots. The winter months are shaded in light blue. Note that sometimes there is no GEDI data in a given month.

In this study we have filtered all granules that were consistently 30 m above or below the global reference surface, using the fields (*geophys_corr/dem_h* for ICESat-2 and *digital_elevation_model* for GEDI) present in the data products. Lower thresholds would also filter out correct data. We identified more erroneous granules, especially for GEDI, but found no clear metric to uniquely identify these granules without removing actual data. Our resulting list of unused granules for the reference areas is supplied in the supplementary materials.

4.2. Spatial coverage and the resolution of global DEMs

While no global DEM based on GEDI exist as of writing, several have been made using ICESat-2. The 1 km DEM of Antarctica by Shen et al. (2021) could be improved to 200 m by using all ICESat-2 data. The GLL_DTM by Vernimmen and Hooijer (2023) using all ICESat-2 data is already at a 1 km resolution. Both these resolutions are already beyond the planned 2 km maximum track seperation as planned by the ICESat-2 mission (Markus et al., 2017). Adding GEDI data to such DEMs (applicable only between 51.6° N and 51.6° S latitude) would further improve the resolution, but lower the precision. This trade-off depends on the slope of the terrain, i.e. whether the error due to the gap in ICESat-2 data is larger than the error due to the lower precision of GEDI.

The achievable global DEM resolution of 500 m by combining ICESat-2 and GEDI is a great step forward for data-scarce areas, but it is still far removed from current available global DEMs at 30 m resolution. However, as pointed out by Bates (2012), current global DEMs measure the elevation of the surface, which is not necessarily the elevation of the terrain. Accurate (airborne) lidar DEMs are currently only available for a small fraction of the globe. Spaceborne lidar DEMs thus are a valuable addition, especially in data-scarce regions with ubiquitous forest cover, such as the tropics, even at a low resolution.

The spatial coverage—after five years of continuous data collection—will still improve during the remaining lifespan of these satellites. GEDI has passed its prime mission phase, and has been put into hibernation on the ISS after a first mission extension. A second mission extension is planned for 2024-2026, and a third extension—if granted—could extend the mission until the deorbit of the ISS in the 2030s (Dubayah, 2023). ICESat-2 has also exceeded its nominal mission duration and could—barring anomalies—even continue to 2036 given the current onboard resources (Kurtz et al., 2023). Both missions would then exceed the lifespan of the first ICESat mission (∼7 years). In this optimistic scenario, we would see a sub 500 m resolution everywhere. For achieving even higher resolutions, a constellation of ICESat-2 like satellites was already proposed by Hancock et al. (2021).

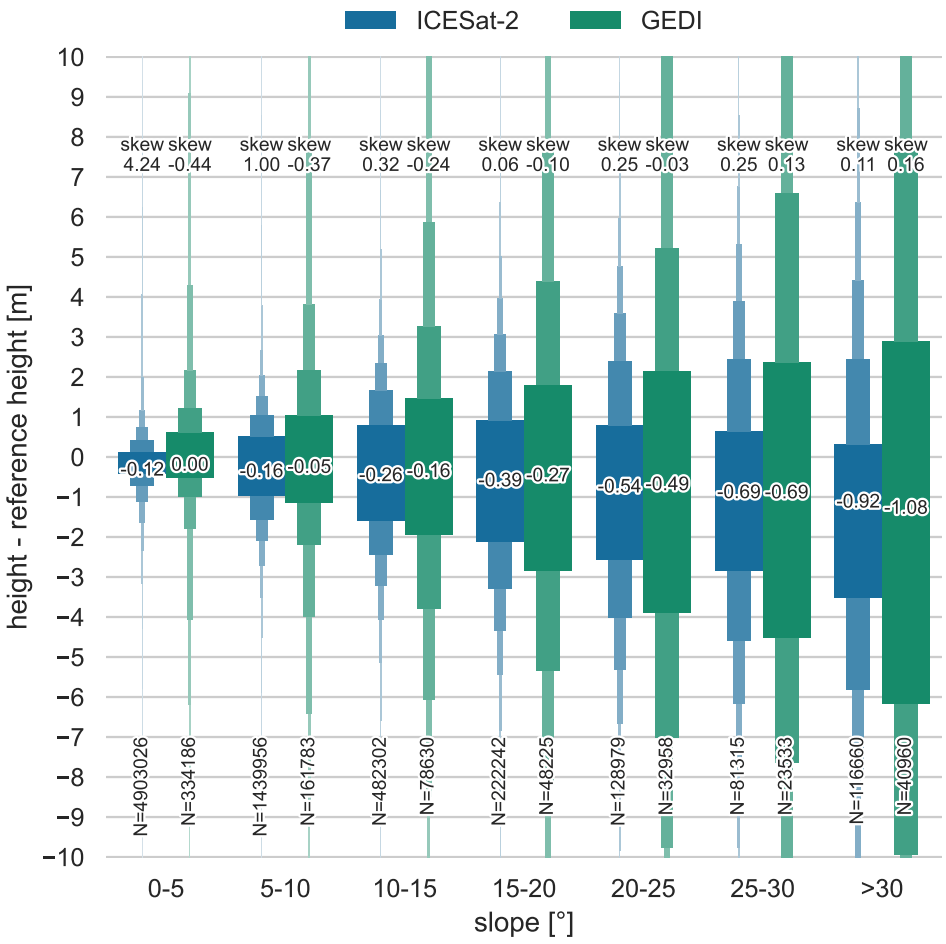

Figure 10: Elevation difference per slope category in Switzerland as boxenplots for both missions compared to reference areas. The skewness, median, and the number of samples is included in the top, middle and lower part of the figure, respectively. Note how an increasing slope has a negative correlation on the accuracy and precision and that GEDI suffers more from this effect than ICESat-2.

4.3. Limitations and overall recommendations

A direct point-to-point comparison between ICESat-2 and GEDI is not straightforward and has not been implemented. As shown in Figure 2 and 11a, the different orbits and beam configurations of the two missions yield few intersections between footprints. After filtering, even fewer points remain, and the number of points is too low to perform an analysis that could relate to environmental factors such as land cover or slope.

In this study we rasterise the ICESat-2 and GEDI samples to assess their spatial coverage, which is an understudied aspect of these sparse datasets. While this gives an upper bound on the resolution of a (global) DEM, we do not seek to create one: it would require more research into combining these two different datasets. Instead, we emphasize that the application of spaceborne lidar is probably more limited by its spatial coverage—depending on the latitude of the area of interest—than its vertical accuracy.

For practical purposes, we note that the data sizes involved can hinder processing. This is especially true for GEDI, and while version 2 was improved by dividing each orbit into four granules, the number of granules and total download size exceeds ICESat-2 while having ∼100 times fewer data points. Similarly, while the filters applied in this study are effective, they are not straightforward to implement (particularly

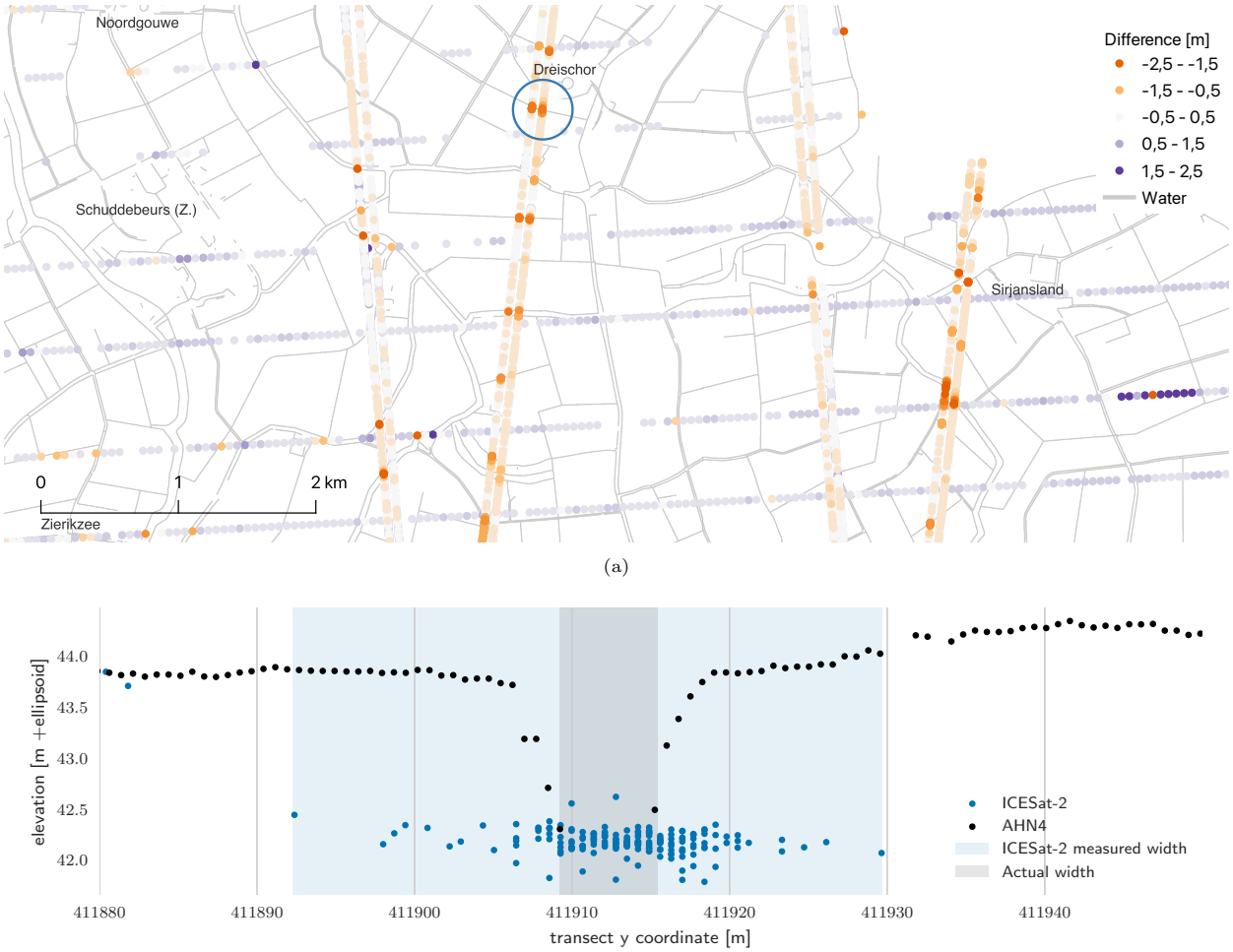

Figure 11: (a) Selection of ICESat-2 and GEDI measurements (not to scale) over Schouwen-Duiveland (near Dreischor and Sirjansland) in the Netherlands, coloured for difference with the Dutch national elevation model. Negative outliers (coloured in orange) most often occur at water bodies (grey lines are rivers, canals, or ditches from TOP10NL). (b) Cross-section of a ditch from (a), indicated with blue circle, with ICESat-2 points and the Dutch national elevation model as reference. ICESat-2 points—actually the centre-points of ∼11 m wide footprints—can exaggerate the width of highly reflective features, such as the water in a ditch. Note the large number of points in the ditch itself as well, indicative of a specular reflection.

so for ICESat-2), and incomplete for detecting all outlier tracks. It must be noted that the data products of ICESat-2 and GEDI are still in development and are subject to improvements.

5. Conclusions

In this study, we validated the terrain measurements of ICESat-2 and GEDI lidar satellites against airborne lidar datasets over three areas in the Netherlands, Switzerland and New Zealand. We used three and a half years of ICESat-2 ATL03 data (2018-10-13 to 2023-10-26) and three years of GEDI L2A data (2019-04-18 to 2023-07-16) for a total of 252 million measurements.

For all areas and land cover classes combined, ICESat-2 achieved a bias of −0.11 m, a MAE of 0.43 m, and a RMSE of 0.93 m (N=236 932 686). We found that GEDI is less accurate with a bias of 0.09 m, a MAE of 0.98 , and a RMSE of 2.96 (N=15 544 899). The difference in the number of samples stems from the higher sampling rate of ICESat-2 compared to GEDI. Measurements in open land cover classes, such as "Cropland" and "Grassland", result in the best precision for both missions. Precision decreases in "Sparse vegetation" areas and is worst in "Tree Cover" for GEDI and in "Built-up" areas for ICESat-2. Both missions are the least accurate in urban areas, as buildings are mistaken for ground, resulting in a strong positive bias of 0.5 m.

We found that the slope of the measured terrain has a major influence on accuracy, and more so for GEDI than ICESat-2. Overall, little effect of either beam power or day-time of measurements was found, nor did we find significant seasonal effects on accuracy. We concluded that the applied filtering is sufficient to remove most outliers for both products. Our results are comparable or better than previous studies, which we also attribute to using newer versions of the data products.

Furthermore, we investigated the current spatial coverage of ICESat-2 and GEDI by deriving a DEM at different resolutions and latitudes. GEDI has higher spatial coverage than ICESat-2 at lower latitudes, due to its beam pattern and lower inclination angle, and can achieve a resolution of 700 m. ICESat-2 only reaches a resolution of 1000 m at the equator, but increases to 200 m at higher latitudes. Finally, we were the first to show that a DEM of 500 m resolution could be achieved globally when ICESat-2 and GEDI are combined.

We provided recommendations on processing both ICESat-2 and GEDI data for DEM creation, especially in terms of filtering outlier tracks. With these filters applied, both ICESat-2 and GEDI enable accurate terrain measurements anywhere in the world. In data-poor areas with ubiquitous forest cover—such as the tropics—these spaceborne lidar instruments enable accurate remote-sensed terrain measurements for the first time. This has considerable potential for new applications and insights, such as estimation of flood risk.

Appendix A. GEDI filtering

The GEDI data are filtered based on the parameters used for the higher level L3A gridded data product. These parameters are described in section 3.3.1 of the GEDI ATBD document (Dubayah et al., 2021c) and are repeated here in Table A.4

Table A.4: Filter parameters used to filter GEDI. Replication of Table 3-2 in the GEDI ATBD document (Dubayah et al., 2021c) for GEDI L3A.

L2A Variable Name	Criteria for Return Inclusion
rx_assess_quality_flag	!= 0
surface_flag	!= 0
stale_return_flag	== 0
rx_maxamp	>8*sd_corrected
sensitivity	<=1 and >0.90
rx_algrunflag	!= 0
zcross	>0
toploc	>0
degrade_flag	== 0

Appendix B. Overview of validation areas

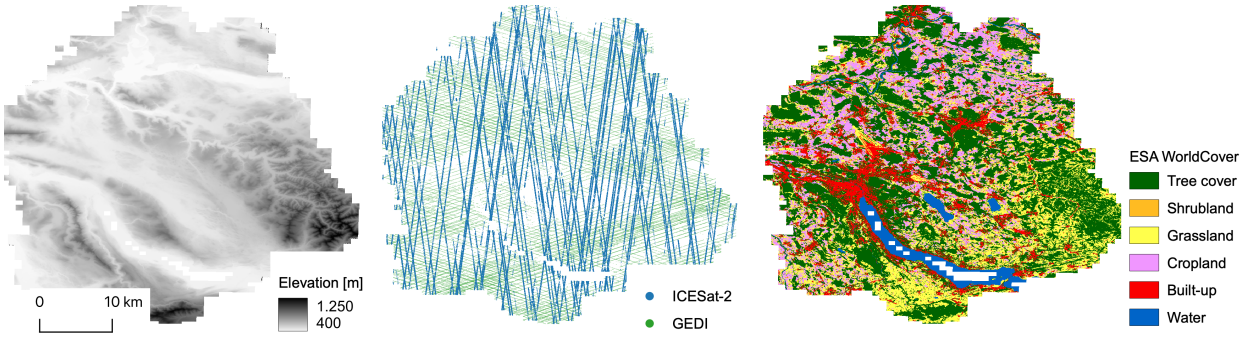

Figure B.12: A visual overview of the datasets used for the reference area in Switzerland.

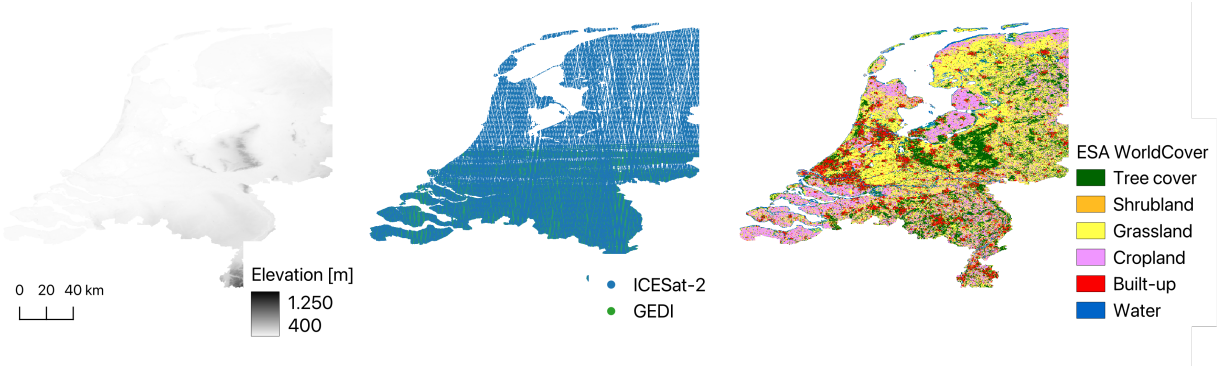

Figure B.13: A visual overview of the datasets used for the reference area in The Netherlands.

Appendix C. Landcover statistics per validation area

Table C.5: Validation with reference areas for each landcover class in The Netherlands

Landcover	bias [m]		MAE [m]		RMSE [m]		number of observations	
	ICESat-2	GEDI	ICESat-2	GEDI	ICESat-2	GEDI	ICESat-2	GEDI
Tree cover	−0.26	0.36	0.52	1.17	0.95	2.85	25 865 997	3 436 318
Built-up	0.65	0.49	1.19	1.08	2.31	2.47	15 696 777	1 013 419
Grassland	−0.19	−0.05	0.38	0.63	0.69	1.36	123 508 586	5 614 243
Bare / sparse vegetation	−0.16	−0.01	0.43	0.91	0.87	2.03	3 192 171	124 853
Cropland	−0.09	0.01	0.27	0.56	0.49	1.41	48 200 309	4 082 031
Herbaceous wetland	−0.24	−0.03	0.31	0.56	0.59	0.93	8 550 489	125 787
All landcovers	−0.11	0.1	0.43	0.77	0.9	1.92	225 014 329	14 396 651

Table C.6: Validation with reference areas for each landcover class in Switzerland

Landcover	bias [m]		MAE [m]		RMSE [m]		number of observations	
	ICESat-2	GEDI	ICESat-2	GEDI	ICESat-2	GEDI	ICESat-2	GEDI
Tree cover	−0.31	0.22	0.66	3.2	1.62	6.6	1 884 941	369 528
Built-up	0.24	0.37	0.81	1.43	2.05	3.54	720 764	48 165
Grassland	−0.2	−0.27	0.37	1.54	0.79	4.12	2 836 089	202 807
Bare / sparse vegetation	−0.63	−0.36	1.16	2.79	3.13	6.68	73 959	4508
Cropland	−0.1	−0.12	0.28	0.86	0.58	2.14	1 833 414	95 070
Herbaceous wetland	−0.25	−0.06	0.28	0.5	0.95	1.33	25 707	228
All landcovers (slope 0° to 5°)	−0.09	0.13	0.35	1.19	0.99	3.31	4 903 026	334 186
All landcovers	−0.17	0.04	0.47	2.3	1.23	5.37	7 374 874	720 306

Table C.7: Validation with reference areas for each landcover class in New Zealand. Note that GEDI has a much higher percentage in tree cover (the worst performing landcover) than ICESat-2, impacting the all landcovers result negatively.

Landcover	bias [m]		MAE [m]		RMSE [m]		number of observations	
	ICESat-2	GEDI	ICESat-2	GEDI	ICESat-2	GEDI	ICESat-2	GEDI
Tree cover	0.14	0.59	1.22	8.62	2.69	16.02	684 995	161 651
Built-up	1.1	−0.23	1.34	2.94	2.8	5.59	432 362	24 580
Grassland	−0.13	−0.65	0.41	4.0	0.9	9.19	3 017 729	226 818
Bare / sparse vegetation	−0.72	−1.86	1.44	6.62	4.59	14.73	94 261	4551
Cropland	−0.03	−0.4	0.3	1.94	0.68	3.93	233 577	9456
Herbaceous wetland	−0.06	0.56	0.31	0.92	0.51	3.23	80 559	886
All landcovers	0.02	−0.16	0.63	5.66	1.68	12.09	4 543 483	427 942

References

Adam, M., Urbazaev, M., Dubois, C., Schmullius, C., 2020. Accuracy Assessment of GEDI Terrain Elevation and Canopy Height Estimates in European Temperate Forests: Influence of Environmental and Acquisition Parameters. Remote Sens. 12, 3948. doi:10.3390/rs12233948.

Bates, P.D., 2012. Integrating remote sensing data with flood inundation models: How far have we got? Hydrol. Process. 26, 2515–2521. doi:10/ghq4wd.

Bezanson, J., Edelman, A., Karpinski, S., Shah, V.B., 2017. Julia: A Fresh Approach to Numerical Computing. SIAM Rev. 59, 65–98. doi:10/f9wkpj.

van Dijk, A., Bos, M.G., 2013. GIS and Remote Sensing Techniques in Land- and Water-management. Springer Science & Business Media.

Dubayah, R., 2023. GEDI past and future: Assessing four years of ecosystem structure observations from NASA's Global Ecosystem Dynamics Investigation, in: AGU23, AGU.

Dubayah, R., Blair, J.B., Goetz, S., Fatoyinbo, L., Hansen, M., Healey, S., Hofton, M., Hurtt, G., Kellner, J., Luthcke, S., Armston, J., Tang, H., Duncanson, L., Hancock, S., Jantz, P., Marselis, S., Patterson, P.L., Qi, W., Silva, C., 2020. The Global Ecosystem Dynamics Investigation: High-resolution laser ranging of the Earth's forests and topography. Sci. Remote Sens. 1, 100002. doi:10/ggjxx8.

Dubayah, R., Hofton, M., Blair, J., Armston, J., Tang, H., Luthcke, S., 2021a. GEDI L2A Elevation and Height Metrics Data Global Footprint Level V002. doi:10.5067/GEDI/GEDI02_A.002.

Dubayah, R., Luthcke, S., Sabaka, T., Nicholas, J., Preaux, S., Hofton, M., 2021b. GEDI L3 gridded land surface metrics, version 1 doi:10/gjn6fv.

Dubayah, R.O., Luthcke, S.B., Sabaka, T.J., Nicholas, J.B., Preaux, S., Hofton, M.A., 2021c. GEDI L3 Gridded Land Surface Metrics, Version 2. ORNL DAAC doi:10.3334/ORNLDAAC/1952.

Funning, G.J., Parsons, B., Wright, T.J., Jackson, J.A., Fielding, E.J., 2005. Surface displacements and source parameters of the 2003 Bam (Iran) earthquake from Envisat advanced synthetic aperture radar imagery. J. Geophys. Res. Solid Earth 110. doi:10.1029/2004JB003338.

Hancock, S., McGrath, C., Lowe, C., Davenport, I., Woodhouse, I., 2021. Requirements for a Global Lidar System: Spaceborne lidar with wall-to-wall coverage. R. Soc. Open Sci. doi:10.1098/rsos.211166.

Hengl, T., Leal Parente, L., Krizan, J., Bonannella, C., 2020. Continental Europe Digital Terrain Model at 30 m resolution based on GEDI, ICESat-2, AW3D, GLO-30, EUDEM, MERIT DEM and background layers. doi:10.5281/zenodo.4724549.

Hofmann, H., Wickham, H., Kafadar, K., 2017. Letter-Value Plots: Boxplots for Large Data. J. Comput. Graph. Stat. 26, 469–477. doi:10/gf38v7.

Hooijer, A., Vernimmen, R., 2021. Global LiDAR land elevation data reveal greatest sea-level rise vulnerability in the tropics. Nat. Commun. 12, 3592. doi:10/gkzf49.

Kurtz, N.T., Fricker, H.A., Neumann, T., 2023. NASA ICESat-2 Mission Status and Highlights, in: AGU23, AGU.

Liu, A., Cheng, X., Chen, Z., 2021. Performance evaluation of GEDI and ICESat-2 laser altimeter data for terrain and canopy height retrievals. Remote Sens. Environ. 264, 112571. doi:10/gkzw4v.

Magruder, L., Neuenschwander, A., Klotz, B., 2021. Digital terrain model elevation corrections using space-based imagery and ICESat-2 laser altimetry. Remote Sens. Environ. 264, 112621. doi:10/gmhzpq.

Magruder, L.A., Farrell, S.L., Neuenschwander, A., Duncanson, L., Csatho, B., Kacimi, S., Fricker, H.A., 2024. Monitoring Earth's climate variables with satellite laser altimetry. Nat Rev Earth Environ , 1–17doi:10.1038/s43017-023-00508-8.

Malambo, L., Popescu, S.C., 2021. Assessing the agreement of ICESat-2 terrain and canopy height with airborne lidar over US ecozones. Remote Sens. Environ. 266, 112711. doi:10/gmxn3k.

Mallet, C., Bretar, F., 2009. Full-waveform topographic lidar: State-of-the-art. ISPRS J. Photogramm. Remote Sens. 64, 1–16. doi:10.1016/j.isprsjprs.2008.09.007.

Markus, T., Neumann, T., Martino, A., Abdalati, W., Brunt, K., Csatho, B., Farrell, S., Fricker, H., Gardner, A., Harding, D., Jasinski, M., Kwok, R., Magruder, L., Lubin, D., Luthcke, S., Morison, J., Nelson, R., Neuenschwander, A., Palm, S., Popescu, S., Shum, CK., Schutz, B.E., Smith, B., Yang, Y., Zwally, J., 2017. The Ice, Cloud, and land Elevation Satellite-2 (ICESat-2): Science requirements, concept, and implementation. Remote Sens. Environ. 190, 260–273. doi:10/gg3f7c.

Masoud, A.A., Koike, K., 2011. Auto-detection and integration of tectonically significant lineaments from SRTM DEM and remotely-sensed geophysical data. ISPRS J. Photogramm. Remote Sens. 66, 818–832. doi:10.1016/j.isprsjprs.2011.08.003.

Meigs, A., 2013. Active tectonics and the LiDAR revolution. Lithosphere 5, 226–229. doi:10.1130/RF.L004.1.

Moudry, V., Lecours, V., Gdulová, K., Gábor, L., Moudrá, L., Kropáček, J., Wild, J., 2018. On the use of global DEMs in ecological modelling and the accuracy of new bare-earth DEMs. Ecol. Model. 383, 3–9. doi:10.1016/j.ecolmodel.2018.05.006.

Neuenschwander, A., Guenther, E., White, J.C., Duncanson, L., Montesano, P., 2020. Validation of ICESat-2 terrain and canopy heights in boreal forests. Remote Sens. Environ. 251, 112110. doi:10/ghdkrh.

Neuenschwander, A., Pitts, K., 2019. The ATL08 land and vegetation product for the ICESat-2 Mission. Remote Sens. Environ. 221, 247–259. doi:10/gf9wmm.

Neuenschwander, A.L., Magruder, L.A., 2019. Canopy and Terrain Height Retrievals with ICESat-2: A First Look. Remote Sens. 11, 1721. doi:10/gf9wmn.

Neuenschwander, A.L., Pitts, K.L., Jelley, B.P., Robbins, J., Klotz, B., Popescu, S.C., Nelson, R.F., Harding, D., Pederson, D., Sheridan, R., 2021. ATLAS/ICESat-2 L3A Land and Vegetation Height, version 5. doi:10.5067/ATLAS/ATL08.005.

Neumann, T.A., Brenner, A., Hancock, D., Robbins, J., Saba, J., Harbeck, K., Gibbons, A., Lee, J., Luthcke, S.B., Rebold, T., 2021. ATLAS/ICESat-2 L2A Global Geolocated Photon Data, version 5. doi:10.5067/ATLAS/ATL03.005.

Neumann, T.A., Martino, A.J., Markus, T., Bae, S., Bock, M.R., Brenner, A.C., Brunt, K.M., Cavanaugh, J., Fernandes, S.T., Hancock, D.W., Harbeck, K., Lee, J., Kurtz, N.T., Luers, P.J., Luthcke, S.B., Magruder, L., Pennington, T.A., Ramos-Izquierdo, L., Rebold, T., Skoog, J., Thomas, T.C., 2019. The Ice, Cloud, and Land Elevation Satellite – 2 mission: A global geolocated photon product derived from the Advanced Topographic Laser Altimeter System. Remote Sens. Environ. 233,

111325. doi:10/ghf8jm.
Okolie, C.J., Smit, J.L., 2022. A systematic review and meta-analysis of Digital elevation model (DEM) fusion: Pre-processing, methods and applications. ISPRS J. Photogramm. Remote Sens. 188, 1–29. doi:10.1016/j.isprsjprs.2022.03.016.
Pronk, M., Gardner, A., 2021. SpaceLiDAR.jl. Zenodo. doi:10.5281/zenodo.7527509.
Pronk, M., Hooijer, A., Eilander, D., Haag, A., de Jong, T., Vousdoukas, M., Vernimmen, R., Ledoux, H., Eleveld, M., 2024. DeltaDTM: A global coastal digital terrain model. Sci Data 11, 273. doi:10.1038/s41597-024-03091-9.
Quiros, E., Polo, M.E., Fragoso-Campon, L., 2021. GEDI Elevation Accuracy Assessment: A Case Study of Southwest Spain. IEEE J. Sel. Top. Appl. Earth Obs. Remote Sens. , 1–1doi:10/gj6rvq.
Schneider, F.D., Ferraz, A., Hancock, S., Duncanson, L.I., Dubayah, R.O., Pavlick, R.P., Schimel, D.S., 2020. Towards mapping the diversity of canopy structure from space with GEDI. Environ. Res. Lett. 15, 115006. doi:10/gg27d9.
Schumann, G.J.P., Bates, P.D., 2018. The Need for a High-Accuracy, Open-Access Global DEM. Front. Earth Sci. 6, 225. doi:10/gnjm7j.
Shen, X., Ke, C.Q., Fan, Y., Drolma, L., 2021. A fine-scale digital elevation model of Antarctica derived from ICESat-2. Cryosphere Discuss. 2021, 1–21. doi:10.5194/tc-2021-204.
Su, J., Bork, E., 2006. Influence of Vegetation, Slope, and Lidar Sampling Angle on DEM Accuracy. Photogramm. Eng. Remote Sens. 72, 1265–1274. doi:10.14358/PERS.72.11.1265.
Thuillier, G., Hersé, M., Labs, D., Foujols, T., Peetermans, W., Gillotay, D., Simon, P., Mandel, H., 2003. The Solar Spectral Irradiance from 200 to 2400 nm as Measured by the SOLSPEC Spectrometer from the Atlas and Eureca Missions. Sol. Phys. 214, 1–22. doi:10.1023/A:1024048429145.
Urbazaev, M., Hess, L.L., Hancock, S., Sato, L.Y., Ometto, J.P., Thiel, C., Dubois, C., Heckel, K., Urban, M., Adam, M., Schmullius, C., 2022. Assessment of terrain elevation estimates from ICESat-2 and GEDI spaceborne LiDAR missions across different land cover and forest types. Sci. Remote Sens. 6, 100067. doi:10.1016/j.srs.2022.100067.
Vernimmen, R., Hooijer, A., 2023. New LiDAR-Based Elevation Model Shows Greatest Increase in Global Coastal Exposure to Flooding to Be Caused by Early-Stage Sea-Level Rise. Earths Future 11, e2022EF002880. doi:10.1029/2022EF002880.
Wake, S., Ramos-Izquierdo, L.A., Eegholm, B., Dogoda, P., Denny, Z., Hersh, M., Mulloney, M., Thomes, W.J., Ott, M.N., Jakeman, H., Poulios, D., Mule, P., de Leon, E., Blair, J.B., 2019. Optical system design and integration of the Global Ecosystem Dynamics Investigation Lidar, in: Infrared Remote Sens. Instrum. XXVII, SPIE. pp. 99–111. doi:10.1117/12.2530653.
Wang, C., Wang, C., Wang, C., Zhu, X., Zhu, X., Zhu, X., Nie, S., Nie, S., Nie, S., Xi, X., Li, D., Zheng, W., Chen, S., 2019. Ground elevation accuracy verification of ICESat-2 data: A case study in Alaska, USA. Opt. Express 27, 38168–38179. doi:10/ggtqmg.
Xing, Y., Huang, J., Gruen, A., Qin, L., 2020. Assessing the Performance of ICESat-2/ATLAS Multi-Channel Photon Data for Estimating Ground Topography in Forested Terrain. Remote Sens. 12, 2084. doi:10.3390/rs12132084.
Yang, L., Meng, X., Zhang, X., 2011. SRTM DEM and its application advances. Int. J. Remote Sens. 32, 3875–3896. doi:10.1080/01431161003786016.
Zanaga, D., Van De Kerchove, R., De Keersmaecker, W., Souverijns, N., Brockmann, C., Quast, R., Wevers, J., Grosu, A., Paccini, A., Vergnaud, S., Cartus, O., Santoro, M., Fritz, S., Georgieva, I., Lesiv, M., Carter, S., Herold, M., Li, L., Tsendbazar, Nandin-Erdene, Ramoino, F., Arino, O., 2021. ESA WorldCover 10 m 2020 v100. doi:10.5281/ZENODO.5571936.
Zhao, P., Li, S., Ma, Y., Liu, X., Yang, J., Yu, D., 2022. A new terrain matching method for estimating laser pointing and ranging systematic biases for spaceborne photon-counting laser altimeters. ISPRS J. Photogramm. Remote Sens. 188, 220–236. doi:10.1016/j.isprsjprs.2022.04.015.
Zhu, X., Nie, S., Wang, C., Xi, X., Hu, Z., 2018. A Ground Elevation and Vegetation Height Retrieval Algorithm Using Micro-Pulse Photon-Counting Lidar Data. Remote Sens. 10, 1962. doi:10.3390/rs10121962.
Zhu, X., Nie, S., Zhu, Y., Chen, Y., Yang, B., Li, W., 2023. Evaluation and Comparison of ICESat-2 and GEDI Data for Terrain and Canopy Height Retrievals in Short-Stature Vegetation. Remote Sens. 15, 4969. doi:10.3390/rs15204969.